Journal of
Experimental
Botany

www.jxb.oxfordjournals.org

RESEARCH PAPER

Morphogenesis at the inflorescence shoot apex of *Anagallis arvensis*: surface geometry and growth in comparison with the vegetative shoot

Dorota Kwiatkowska[1],* and Anne-Lise Routier-Kierzkowska[2]

[1] Department of Biophysics and Morphogenesis of Plants, University of Silesia, Jagiellońska 28, 40-032 Katowice, Poland
[2] Institute of Plant Biology, University of Wrocław, Kanonia 6/8, 50-328 Wrocław, Poland

Abstract

Quantitative analysis of geometry and surface growth based on the sequential replica method is used to compare morphogenesis at the shoot apex of *Anagallis arvensis* in the reproductive and vegetative phases of development. Formation of three types of lateral organs takes place at the *Anagallis* shoot apical meristem (SAM): vegetative leaf primordia are formed during the vegetative phase and leaf-like bracts and flower primordia during the reproductive phase. Although the shapes of all the three types of primordia are very similar during their early developmental stages, areal growth rates and anisotropy of apex surface growth accompanying formation of leaf or bract primordia are profoundly different from those during formation of flower primordia. This provides an example of different modes of *de novo* formation of a given shape. Moreover, growth accompanying the formation of the boundary between the SAM and flower primordium is entirely different from growth at the adaxial leaf or bract primordium boundary. In the latter, areal growth rates at the future boundary are the lowest of all the apex surface, while in the former they are relatively very high. The direction of maximal growth rate is latitudinal (along the future boundary) in the case of leaf or bract primordium but meridional (across the boundary) in the case of flower. The replica method does not enable direct analysis of growth in the direction perpendicular to the apex surface (anticlinal direction). Nevertheless, the reconstructed surfaces of consecutive replicas taken from an individual apex allow general directions of SAM surface bulging accompanying primordium formation to be recognized. Precise alignment of consecutive reconstructions shows that the direction of initial bulging during the leaf or bract formation is nearly parallel to the shoot axis (upward bulging), while in the case of flower it is perpendicular to the axis (lateral bulging). In future, such 3D reconstructions can be used to assess displacement velocity fields so that growth in the anticlinal direction can be assessed. In terms of self-perpetuation, the inflorescence SAM of *Anagallis* differs from the SAM in the vegetative phase in that the centrally located region of slow growth is less distinct in the inflorescence SAM. Moreover, the position of this slowly growing zone with respect to cells is not stable in the course of the meristem ontogeny.

Key words: *Anagallis arvensis*, bract primordium, flower primordium, geometry, growth, shoot apical meristem.

Introduction

A major function of the shoot apical meristem (SAM) is formation of lateral organs, such as leaves and axillary shoots. The identity of these organs depends on the phase of shoot development. The transition from the vegetative to the reproductive developmental phase is also accompanied by changes in another process taking place at the SAM, i.e. its self-perpetuation (meaning the maintenance of the size and general shape of the SAM). In particular, division and growth rates of the meristem cells increase (reviewed in Cutter, 1971; Lyndon, 1998). Profound changes occur

in cases of shoots with terminal flowers, e.g. *Datura stramonium* L. (Corson, 1969), capitulum inflorescence, such as in sunflower *Helianthus annuus* L. (Marc and Palmer, 1984), or inflorescence with a sympodial type of branching as in *Silene coeli-rosa* L. Gordon (Lyndon, 1998). Moreover, in these cases, after the transition to the reproductive phase of development growth of the SAM becomes determinate and axial extension of the shoot soon ceases. In contrast, in plants with a racemose type of inflorescence, bracts replace vegetative leaves while flowers are formed in the bract axils. The SAM growth often remains indeterminate for a considerable number of plastochrons until eventually the terminal flower is formed. This is the case for the model plant *Arabidopsis thaliana* (L.) Heynh. producing flowers in axils of cryptic bracts (Long and Barton, 2000; Hepworth *et al.*, 2006; Kwiatkowska, 2006). In *Anagallis arvensis* L. (Myrsinaceae) the inflorescence is an anthoclade where bracts are leaf-like and each bract subtends a single flower (Weberling, 1989). The inflorescence type is a frondose raceme (Weberling, 1989) of virtually indeterminate axial growth (Tooke *et al.*, 2005), closely resembling a vegetative shoot—the difference being mainly in replacement of vegetative axillary shoots by flowers (Green *et al.*, 1991). Moreover, the *Anagallis* meristem easily reverts to vegetative development upon short-day conditions, a phenomenon that has been extensively studied by Brulfert (Brulfert *et al.*, 1985; Battey and Lyndon, 1990).

Another process accompanying the transition from the vegetative to reproductive phase is structural reorganization of the SAM (Lyndon and Battey, 1985; Bernier, 1988; Kwiatkowska, 2008) that affects the SAM zonation, shape, and mitotic activity. In the majority of vegetative SAMs the cytohistological zones are distinguished by differences in their mitotic activity (Romberger *et al.*, 1993). The central zone is the least active zone while the rib meristem and the peripheral zone are characterized by higher mitotic activity. In the reproductive (inflorescence or terminal flower) SAM the activity of the central zone often strongly increases and the zonation described above is replaced by the mitotically active meristematic mantle overlaying the less active core (Lyndon and Battey, 1985; Bernier, 1988). However, in some plants, the central zone of lower mitotic activity can still be recognized in the inflorescence SAM, as in *Arabidopsis*, though the observed zonation is less profound than in the vegetative phase (Vaughan, 1955; Laufs *et al.*, 1998; reviewed in Kwiatkowska, 2008).

Anagallis arvensis is an obligatory long-day plant (Ballard, 1969; Brulfert *et al.*, 1985). Phyllotaxis of *Anagallis* shoots in the vegetative phase is most often decussate and rather stable, while in the reproductive phase there is a high probability that it changes to a spiral Fibonacci pattern and sometimes further into trimerous whorled phyllotaxis. These changes do not coincide with the transition to the reproductive phase (Kwiatkowska, 1995).

The cellular pattern and cell divisions at the surface of the *Anagallis* shoot apex in the vegetative phase have been studied by Green *et al.* (1991) with the aid of the sequential replica method. Phyllotaxis of these apices was decussate. Vegetative apices exhibiting spiral Fibonacci phyllotaxis have been studied with the same method followed by a quantitative analysis of morphogenesis at the shoot apex (Kwiatkowska and Dumais, 2003). In the latter study, data obtained with the aid of sequential replicas were used for quantification of local geometry of the shoot apex by means of curvature directions (i.e. those directions in which surface curvature is either minimal or maximal) and Gaussian curvature characterizing the overall surface curvature. Furthermore, principal growth directions (the directions on the apex surface in which growth rates attain either maximal or minimal values) and areal growth rates were computed.

The investigations based on the sequential replica method revealed that the growth pattern on the apex changes in time and space, and enabled recognition of early stages of leaf primordium development. In the case of spiral Fibonacci phyllotaxis, the central part of the SAM surface is characterized by slow and nearly isotropic growth and most probably corresponds to the surface of the central zone (Kwiatkowska and Dumais, 2003). Infrequent cell divisions and relatively slow expansion have also been observed at the central SAM part in the decussate vegetative SAM of *Anagallis* (Green *et al.*, 1991). Growth distribution at the SAM periphery is not uniform in plants, showing both decussate and spiral phyllotaxis (Green *et al.*, 1991; Kwiatkowska and Dumais, 2003). In the latter case, the SAM periphery can be divided into wedge-like segments. Their growth pattern depends on the position of the segment and the age of the adjacent leaf primordium. In segments where the SAM periphery is being rebuilt, i.e. those contacting older leaf primordia, areal growth rates and growth anisotropy are higher than in segments contacting younger leaf primordia, not yet separated from the SAM by a distinct boundary (a crease). Sites of new primordium formation are characterized by high growth rates and nearly isotropic growth (the stage of initial bulging). A new primordium is a more or less rounded bulge. Next, growth rates become lower, growth more anisotropic, and the shape of the primordium changes to more oval (the stage of lateral expansion). During the following stage, the separation stage, the primordium becomes separated from the SAM by a saddle-shaped crease. The crease is a future leaf axil, i.e. the adaxial boundary of the primordium. During the next stage, the leaf primordium curves and starts to grow over the SAM (Kwiatkowska and Dumais, 2003).

In the same paper by Green *et al.* (1991) where sequential replicas were used to study cell divisions at the vegetative *Anagallis* apex, the apex in the reproductive phase, exhibiting decussate phyllotaxis, was also studied. In the reproductive phase the flower primordium is formed at the *Anagallis* SAM periphery in the axil of the leaf-like bract primordium. The central region of the inflorescence SAM is characterized by lower mitotic activity than the peripheral region, similar to the vegetative SAM. The anisotropy of growth becomes more pronounced (higher meridional

growth rate, i.e. stronger directional growth) in the peripheral region of the meristem than in the vegetative phase. The flower primordium originates from a narrow row of cells located along the adaxial boundary of a bract primordium, but the area of rapid peripheral extension that accompanies flower primordium formation includes a flower primordium, its adaxial boundary (referred to as a crease by Green *et al.*, 1991), and also the recovering (rebuilding) portion of the SAM. The plastochron is shorter in the reproductive than in the vegetative phase (Green *et al.*, 1991). Since the quantification of geometry and growth has not been performed for *Anagallis* shoot apices in the reproductive phase, this became the purpose of the present investigation.

Exhibiting such rather subtle differences in the shoot morphogenesis between the vegetative and reproductive phases (leaf-like bracts, almost indeterminate growth in the reproductive phase, apparent cytohistological zonation in both the phases), *Anagallis* requires an adequate method for studying differences in SAM function between the two phases, i.e. differences in both its self-perpetuation and early stages of lateral primordium formation. Therefore, the objectives of the present study were to analyse quantitatively growth and geometry changes in the reproductive shoot apex of *Anagallis* with protocols accounting for complex shape and anisotropic growth, and to compare these characteristics of the reproductive apex with already available data for the vegetative apex. One can ask why such a comparison has not been done for the model species *Arabidopsis*. This is because data collection with the employed technique is extremely difficult for a vegetative SAM hidden in the rosette of leaves. Thus only data on the reproductive phase are available for *Arabidopsis* (Kwiatkowska, 2004*a*, 2006).

Materials and methods

Plant material and growth conditions

For the present study, the same strain of *A. arvensis* was used as that described earlier by Kwiatkowska (1997). The plants were propagated by cuttings from the wild plant growing in the Sudety Mountains, Poland. This particular strain has been shown to undergo changes in the phyllotactic pattern in individual shoot ontogeny more often than the other strains studied. Consequently, the frequency of shoots with spiral Fibonacci phyllotaxis in these plants is very high, especially in the reproductive phase of development.

Plants were grown in a growth room with continuous light, temperature ranging between 17 °C and 22 °C, and illumination of 9 W m^{-2}. All the shoot apices selected for the analysis exhibited spiral Fibonacci phyllotaxis, with the angle between consecutively formed leaf primordia (divergence angle) equal to ~137°.

In order to facilitate a comparison between apices in the reproductive and vegetative phase of development, micrographs taken from replicas of shoot apices in the vegetative phase that were earlier used for the growth and geometry analysis described by Kwiatkowska and Dumais (2003) have been used in the present investigation for computations with the aid of a new protocol for stereoscopic reconstruction (Routier-Kierzkowska and Kwiatkowska, 2008) described below. Some of these plants were from the same strain from the Sudety Mountains, while others originated from a plant growing on the Stanford University campus.

Data collection

The sequential replica method has been performed according to an already described protocol (Williams and Green, 1988; Williams, 1991; Dumais and Kwiatkowska, 2002). In this method, replicas (dental polymer moulds) are taken from the individual shoot apex surface at consecutive instants, and scanning electron microscopy (SEM; LEO435VP) is employed for observation of sputter-coated epoxy resin casts. For each cast, two SEM micrographs were taken, one tilted by 10° with respect to the other, in order to facilitate the stereoscopic reconstruction.

Sequences of replicas were taken from five individual apices at 20–48 h intervals for 48–145 h. Since the growth and geometry have been quantified previously for vegetative shoot apices of *Anagallis* exhibiting spiral Fibonacci phyllotaxis, inflorescence apices of the same phyllotaxis were chosen for the present analysis and comparison.

Quantitative analysis of surface geometry and growth

The quantitative analysis comprised three steps: the stereoscopic reconstruction of the apex surface so that it can be defined by the 3D coordinates of vertices (points at which three anticlinal walls of adjacent cells contact); computation of curvature of the apex surface; and computation of growth rates. For the first step, i.e. the stereoscopic reconstruction, a recently described protocol was employed (Routier-Kierzkowska and Kwiatkowska, 2008). Protocols for the computation of curvature and growth rates were the same as described earlier by Dumais and Kwiatkowska (2002). Computer programs used for this analysis have been written in Matlab (The Mathworks, Natick, MA, USA) and are available from the authors upon request.

In the new stereoscopic reconstruction protocol, an automatic dense matching of the two stereo micrographs taken from each replica is employed. It is followed by a triangulation step (Routier-Kierzkowska and Kwiatkowska, 2008). In this way the smooth surface of the replica is reconstructed, taking into account slight differences in magnification between the two micrographs that could lead to erroneous 3D reconstructions. Cell outlines (the connected cell vertices) are digitized on one of the micrographs, and projected on the reconstructed 3D apex surface.

Such coordinates of the vertices are further used for the curvature computation by means of curvature directions and Gaussian curvature. These variables are computed for
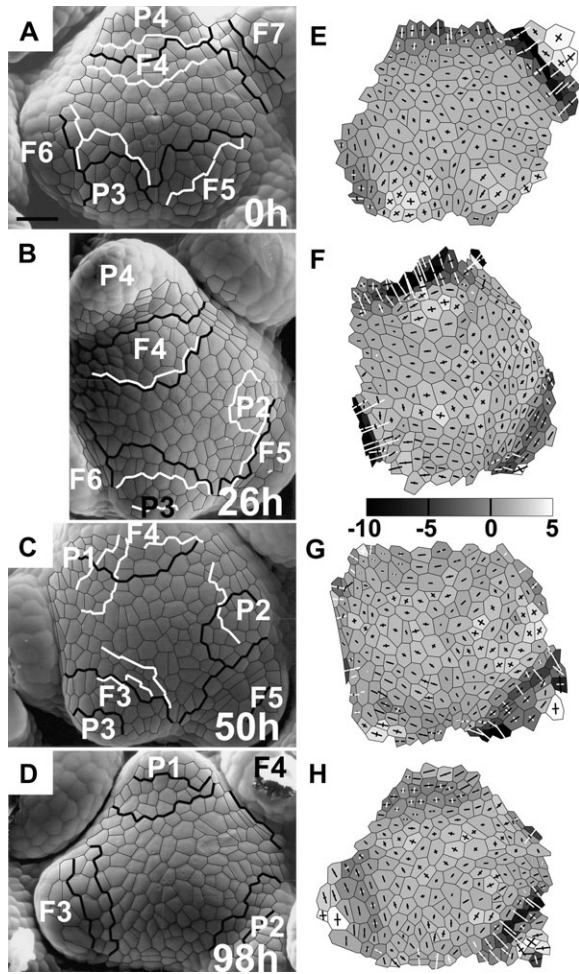
Fig. 1. The developmental sequence of an inflorescence shoot apex of *Anagallis arvensis* illustrating all the stages of the development of the bract primordium (primordium labelled as P3) and the flower primordium emerging in its axil (F3). Scanning electromicrographs (A–D) and curvature plots (E–H) are shown for the sequence of four replicas. The time at which the replica was taken is given in the lower right corner of each micrograph. Bract primordia are labelled with P and a number (the younger the primordium, the lower the number). The flower primordium emerging in the axil of P is labelled by an F with the same number as the P. Each primordium has the same number for the whole sequence of replicas so that a given primordium can be easily followed in consecutive images. Cells used for curvature computation are outlined in black in the micrographs. Gaussian curvature is shown in grey-scale maps, while crosses represent curvature directions. The black cross arm points to the direction in which the surface is convex; the white cross arm to the direction in which it is concave. Arm length is proportional to curvature in the given direction. The scale for Gaussian curvature is in $10^{-4} \ \mu m^{-2}$. Lines overlaid on micrographs show adaxial boundaries of bract or flower primordia, recognized on the basis of curvature. Black lines are boundaries between the SAM and primordia recognized on curvature plots of the given replica; white lines are boundaries recognized on the curvature of the next replica. The boundary is described by two lines if it is the region of nil (e.g. boundary of P3 in C, G) or negative (e.g. boundary of F3 in D, H) Gaussian curvature. Bar=30 μm.

every surface, approximating a group of vertices of a given cell and its direct neighbours, i.e. not for an outer periclinal wall of an individual cell (Dumais and Kwiatkowska, 2002). In the figures, principal curvature directions are represented by crosses, where cross arms point to the curvature directions and arm lengths are proportional to given curvature values. The Gaussian curvature is presented in grey-scale maps.

Growth variables (principal growth directions and areal growth rates) are computed on the basis of recognition of the same vertices in consecutive replicas (Dumais and Kwiatkowska, 2002). In the figures, principal growth directions are represented by crosses with arms pointing to principal directions and arm lengths proportional to growth rates in these directions. Areal growth rates are presented in colour maps.

Dense 3D reconstructions of the replica surface are also used to produce side views (profiles) of apices (Routier-Kierzkowska and Kwiatkowska, 2008). In order to compare side views of consecutive replicas taken from an individual apex, the reconstructions need to be properly aligned. This has been done by fixing the position of a selected referential region of the meristem and allowing the remaining apex portion to 'move freely' with respect to the referential region (the movement is due to growth taking place during a given time interval). The referential region was a group of 7–10 cells of the meristem surface, which were not dividing during the considered time interval and were situated at the apex tip, thus corresponding roughly to the central zone. The two consecutive reconstructions of the given apex were rotated and translated so that the position of the referential region remained fixed. In practice, this meant that a rotation and translation had to be found that brought the centres of the selected cells on the second reconstruction as close as possible to the corresponding cell centres on the first reconstruction. This was achieved by minimizing the sum of squared pairwise distances between cell centres, using a singular value decomposition approach (Arun *et al.*, 1987).

In order to compare the formation of leaf, bract, and flower primordia in vegetative and inflorescence shoot apices of *Anagallis*, the available data on the earlier studied replica sequences from the vegetative developmental phase (Kwiatkowska and Dumais, 2003) were also considered. The dense reconstruction protocol has been applied to these sequences, so that side views of apices at consecutive instants could be analysed.

Results

Formation of the leaf-like bract primordium

Early stages of bract primordium development distinguished on the basis of curvature: Early development of the bract primordium at the reproductive *Anagallis* apex can be divided into distinct stages differing in their geometry. The first stage detectable with the employed protocol for

curvature computation is the bulging at the meristem periphery (the stage of initial bulging). The initial bulging leads to the formation of a region of increased Gaussian curvature, as at the site of P3 formation in Fig. 1A and E. The lengths of two cross arms pointing to the curvature directions at this site are similar, which means that curvature is similar in all the directions as on the surface of a hemisphere. This stage lasts for about half the plastochron. The following stage is the lateral expansion of the primordium (see the same primordium P3 in Fig. 1B and F, i.e. 26 h later). During this stage, the bract primordium outline changes to be more ovate, extended along the latitudinal direction of the SAM. The duration of the lateral expansion stage is again approximately half the plastochron. The adaxial boundary of the bract primordium, assessed during these two stages on the basis of curvature, is not stable with respect to cells (compare the boundary of P3 in Fig. 1A and B). The boundary during these two stages is, however, not distinct.

During the next stage, the bract primordium is separated from the SAM (the separation stage). This leads to formation of a distinct, saddle-shaped crease between the primordium and SAM, i.e. the future bract axil. The crease is usually composed of two to three latitudinal rows of cells. It is concave in the meridional direction and convex in the latitudinal direction (like the axil of P3 in Fig. 1C, G; or P3 in Fig. 2A, B, D, E). The duration of the separation stage is again about half the plastochron. Cells contributing to formation of the crease are the cells assigned to the bract primordium at the earlier developmental stage and often also SAM cells adjacent to the primordium (compare P3 in Fig. 1A, E and C, G; and P2 in Fig. 2B, E and C, F). During the separation stage, the bract primordium attains a flattened shape. Once the saddle-shaped crease, i.e. the future axil, is formed, flower primordium formation begins.

Plastochron duration in the examined apices can be estimated by comparing primordia on consecutive images from the same apex. For example, the developmental stages and sizes of primordia P2 and F4 in Fig. 2C are very similar to those of P3 and F5 in Fig. 2B, respectively. Since P3 and F5 are one plastochron older than P2 and F4 and the time interval between the two replicas shown in Fig. 2B and C is 48 h, the plastochron is ~48 h. Similarly, P3 and F5 in Fig. 1C are slightly more advanced than P4 and F6 in Fig. 1A, and the time interval between these two replicas is 50 h. In only one case out of the five shoot apices studied was a single plastochron (the last in the sequence) ~24 h (compare primordia P1 and F3 in Fig. 1D with two plastochrons older P3 and F5 in Fig. 1C, which was obtained 48 h earlier). This acceleration of morphogenesis may possibly be an early manifestation of phyllotaxis transition from spiral Fibonacci to trimerous whorled pattern known to occur in some reproductive *Anagallis* shoots.

Growth rates accompanying bract primordium formation: The consecutive stages of bract primordium development exhibit characteristic growth patterns. During the stage of
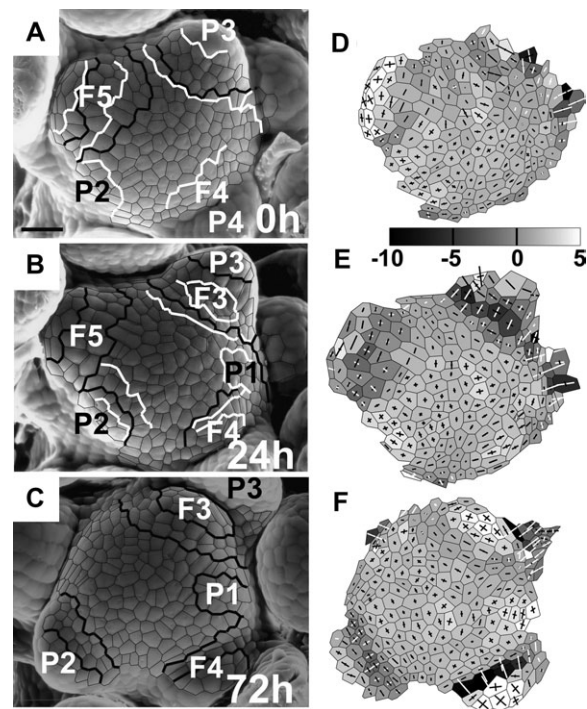

Fig. 2. The developmental sequence of a second inflorescence shoot apex of *Anagallis arvensis* exhibiting spiral Fibonacci phyllotaxis, illustrating the earliest stages of bract primordium development (primordium P2) and the origin of flower primordium (primordium F3). Scanning electromicrographs (A–C) and curvature plots (D–F) for the sequence of three replicas are shown. Labelling as in Fig. 1. Bar=30 μm.

initial bulging, areal growth rates at the site of primordium formation are similar or higher than in the surrounding cells (P1 in Fig. 3A, B, D). Growth is rather anisotropic at the primordium flanks and less anisotropic at the top of the emerging protrusion. Growth rates are lower during the next, lateral expansion stage, while the direction of maximal growth rate tends to be latitudinal (compare growth of the older primordium of the same apex; P2 in Fig. 3A, B, D).

During the following stage, the separation stage, the future axil region is characterized by low areal growth rates and high anisotropy, with a latitudinal direction of maximal growth rate and nearly null growth in the meridional direction (axils of P1 in Fig. 4B, C, E; P3 in Fig. 3G, H, K). In the course of this stage, areal growth rates over the remaining bract primordium surface are higher. Growth of this remaining primordium surface is less anisotropic than at the future axil (compare the adaxial and abaxial parts of P1 in Fig. 3E).

The growth pattern of the bract primordium also remains similar to those described above during flower primordium formation (P3 in Fig. 3A, B, D). Then growth of the axil between the bract primordium and the emerging flower primordium is anisotropic, with the maximal growth rate in the latitudinal direction (along the axil) and a null or negative (contraction) growth rate in the meridional direction (across the axil).
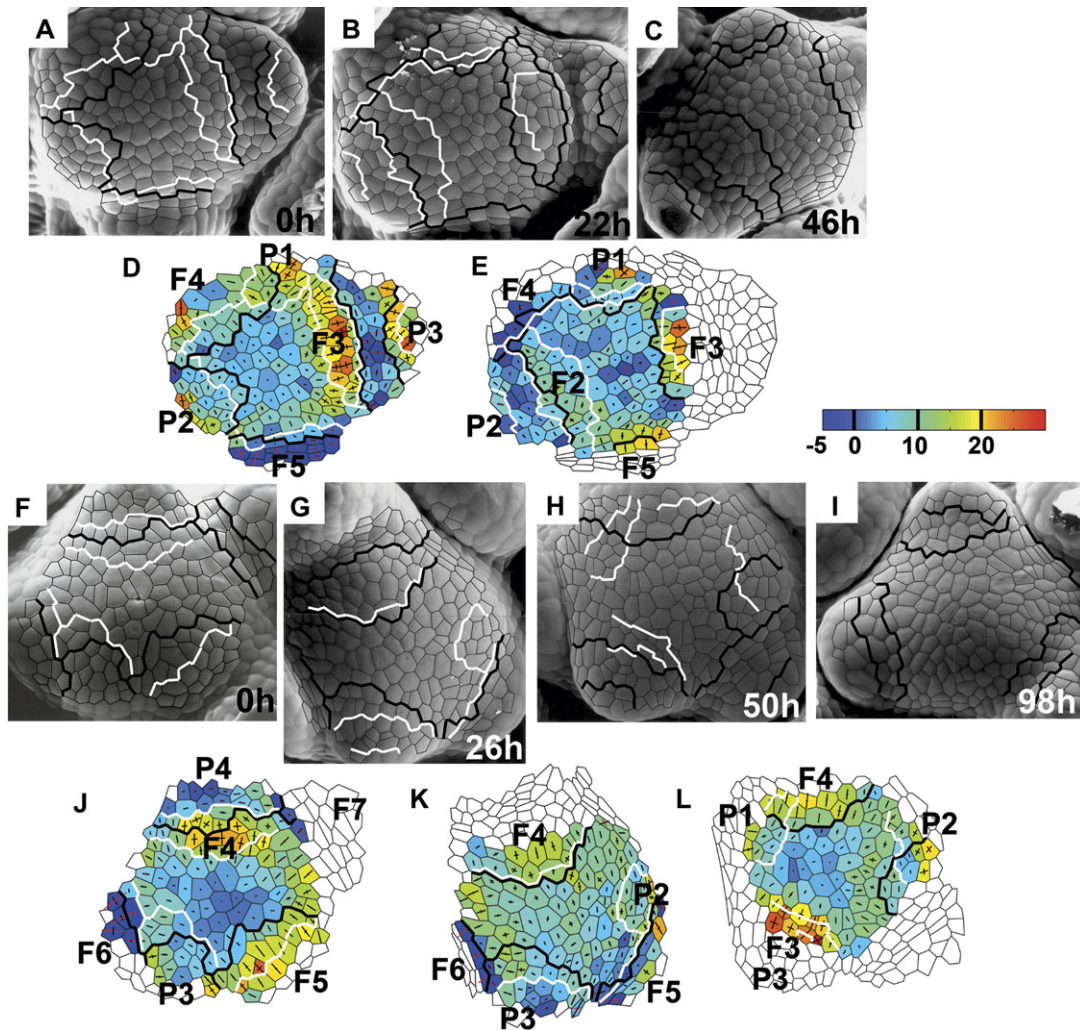
Fig. 3. Growth rates of two individual shoot apices. One of them (F–L) is also shown in Fig. 1. Scanning electromicrographs are presented together with corresponding colour maps representing growth taking place during each time interval. The time at which the replica was taken is given in the lower right corner of each micrograph. Labels (primordia numbers and boundaries) are the same as in Fig. 1. Colour maps representing areal growth rates are plotted on the cell pattern as it appeared at the beginning of the given time interval. The areal growth rate scale is in 10^{-3} h^{-1}. Crosses represent principal growth rates directions; the length of cross arms is proportional to the growth rate in this direction. Arms appear in red if contraction takes place in this direction.

Formation of flower primordium

Early stages of flower primordium development distinguished on the basis of curvature: The first signs of flower primordium formation can be traced on the curvature plots just after the future axil (the crease) of the bract primordium is formed (compare P4, F4 in Fig. 1A, E and B, F). The flower primordium appears first as a lateral protrusion (i.e. a protrusion in the direction nearly perpendicular to the shoot axis), thus the stage will be referred to here as lateral bulging. The flower primordium is then a ridge bent only in a latitudinal direction (i.e. with nearly zero meridional curvature and positive curvature in the latitudinal direction), topped with a hemisphere-like cap, as in the case of F4 in Fig. 1B, F. The flower primordium is formed by SAM cells adjacent to the bract axil together with a portion of the adaxial slope of the bract axil (compare P3/F3 in Fig. 2B, E and C, F). This portion of the bract axil changes its shape

from saddle (negative Gaussian curvature) to nearly hemispherical (positive Gaussian curvature) as exemplified by emerging flower primordium F3 in Fig. 2B, E and C, F. At the same time, the boundary between the bract primordium and the flower primordium, originating from the abaxial part of the bract axil, remains saddle shaped. During this stage, a boundary between the flower primordium (lateral protrusion) and the SAM cannot be easily delineated (e.g. adaxial boundary of F4 in Fig. 1B, F). The stage of lateral bulging takes about half the plastochron. The subtending bract primordium is then about two plastochrons old (e.g. P4 in Fig. 1A, B).

During the next half of the plastochron, the flower primordium gradually becomes separated from the SAM, first by a narrow region flat in the meridional direction and convex in the latitudinal direction (e.g. F5 in Fig. 2A, D, or F3 in Fig. 2C, F). The rows of SAM cells that together with the adjoining bract axil cells participated in flower primordium
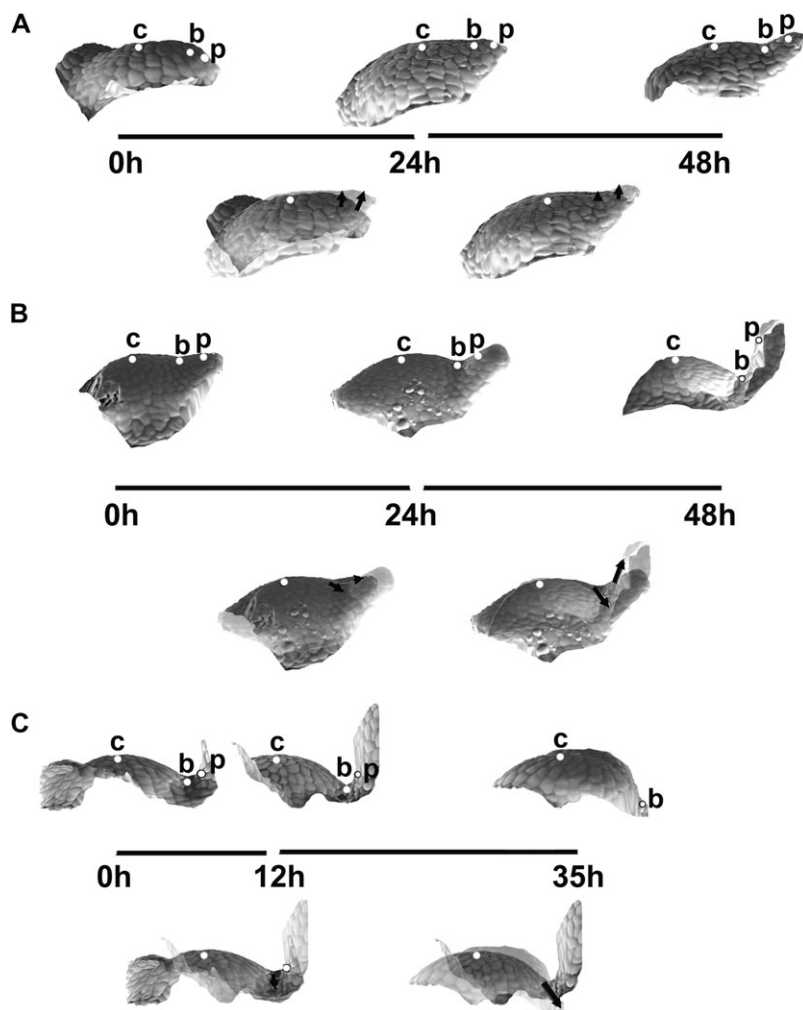
Fig. 4. Sequences of 3D reconstructions of replicas taken from three individual shoot apices of *Anagallis arvensis* in the vegetative developmental phase, representing consecutive stages of leaf primordium development: initial bulging, lateral expansion, and separation stages (A); the separation stage followed by the early stage of primordium curving (B); further curving of the primordium (C). Images in the upper rows of A, B and C are side views of the reconstructed apex surface obtained from consecutive replicas. The time at which the replicas were taken is given below each reconstruction; the length of line segments between the reconstructions is proportional to the time interval between the consecutive replicas. White dots labelling the profiles point to these same cells recognized on the replicas: c is the cell on the top of SAM; b is the cell at the boundary between the meristem and leaf primordium; and p is the cell on the primordium tip or flanks. Images below the 'time segments' are the two consecutive reconstructions overlaid using the protocol described in the text. Arrows connect the positions of each dot in the two overlaid profiles, thus pointing to the displacement directions.

formation often contribute to this boundary formation (compare the boundary of F3 in Fig. 2B, C). This stage will be called the early flower separation stage. The boundary soon becomes more distinct as it attains a saddle-like shape after half the plastochron (compare the above-mentioned flower primordium F5 in Fig. 2A, D with B, E where the region previously bent almost exclusively in the latitudinal direction changes into a saddle, concave in the meridional direction). This stage will be referred to as the late flower separation stage. Finally, the rather wide and shallow saddle-like boundary region begins to deepen and a distinct narrow axil is formed, while a primordium becomes a hemisphere-like bulge pointing in the upward direction (compare F5 in Fig. 1B, F and C, G). This stage, called the deepening of the flower primordium axil, again takes about half the plastochron.

Later stages of flower primordium formation were not followed.

Growth rates accompanying flower primordium formation: The growth pattern at the site of flower primordium formation is very characteristic. During the lateral bulging stage, areal growth rates at the part of the SAM adjacent to the recently formed bract axil are relatively very high. Growth in this region is initially nearly isotropic (F4 in Fig. 3F, G, J), but soon it becomes strongly anisotropic, with the maximal growth rate in the meridional direction, similar in all the cells contributing to the protrusion (compare growth of the same primordium in the consecutive time interval; F4 in Fig. 3G, H, K). This region of fast growth covers more of the SAM surface than later

contribututions to the flower primordium (compare the F3 formation site in Fig. 3A–C with the growth distribution in Fig. 3D, E), i.e. it includes an adjacent portion of the SAM periphery. A similar growth pattern persists during the early and late separation stages (F5 in Fig. 3F, G, J), until the saddle-shaped boundary is formed. During deepening of the flower primordium axil, the growth pattern becomes more complex (compare the same primordium after the next time interval; F5 in Fig. 3K). Cells of the deepening axil grow with low areal growth rates and highly anisotropically, with the maximum growth rate in the nearly latitudinal direction and slight contraction or null growth rate in the meridional direction (e.g. F5 in Fig. 3D). The flower primordium bulge is in turn characterized by high areal growth rates and lower anisotropy, with the maximum growth rate prevalently in the meridional direction (F5 in Fig. 3K).

It should be kept in mind that only growth in the apex surface is accounted for with the present protocol, so the anisotropy computation does not account for the direction perpendicular to the apex surface.

Self-perpetuation of the inflorescence SAM

Areal growth rates at the central part of the inflorescence SAM surface are generally lower and less anisotropic than on the SAM periphery (Fig. 3). It should be stressed, however, that the region of slow growth is often not located exactly around the centre of the SAM (e.g. Fig. 3L) and it sometimes changes its position with respect to cells in the course of SAM ontogeny (compare Fig. 3J, K, L).

Growth of the SAM periphery is generally faster than in the central region, and not uniform. It is convenient to differentiate the periphery into wedge-like regions, each in contact with a lateral organ primordium of different type and developmental stage (e.g. the SAM periphery in Fig. 3J). The growth pattern of such defined wedge-like regions seems to be correlated with the developmental stage of the adjacent bract or flower primordium. The region of the periphery contacting a bract primordium just before its separation from the SAM exhibits rather low areal growth rates (adjacent to P3 in Fig. 3F, G, J). Growth in this region is anisotropic. The direction of the maximal growth rate is not uniform in the cells, though the latitudinal direction prevails. Areal growth rates in the region neighbouring the already separated bract primordium are higher. Since flower primordium formation begins at this stage, it is hard to delineate the SAM periphery from the flower primordium (the flower primordium has no distinct adaxial boundary until the separation). Before the separation the periphery adjacent to the flower primordium is characterized by generally high areal growth rates and rather anisotropic growth, with a meridional direction of the maximal growth rate (adjacent to F3 in Fig. 3D; F5 in Fig. 3J). Also, after the flower primordium is separated, the adjacent peripheral region exhibits high areal growth rates with strong anisotropy and meridional maximal growth direction (adjacent to F7 in Fig. 3J).

3D reconstructions of the shoot apex surface at consecutive stages of primordium development—comparison between the vegetative and reproductive phase

Analysis of the reconstructed side views of an individual apex surface at consecutive time intervals provides additional information on changes in general apex shape and indirect information on growth of the apex interior, e.g. in the course of bulging of the apex surface that takes place during primordium formation.

During the initial bulging and lateral expansion stages of primordium formation of a vegetative leaf (Fig. 4A, the first two reconstructions) changes in the apex profile are both at the primordium formation site and on the adjacent portion of SAM periphery. The outline of the SAM flanks changes from gently curved to shelf-like. Since the distance from the meristem centre (a dot marked with 'c' in the figure) to the future primordium boundary (dot 'b') virtually does not change, the local growth in the meridional direction is very small. At the same time, the distance from the future primordium boundary to the cell located at the future primordium tip (dot 'p') is increasing, which is a manifestation that here the local growth is stronger. Both of the cells, the one located at the future boundary and the primordium tip cell, are strongly displaced upward. This presumably results from growth in the anticlinal direction on the meristem periphery. It is especially strong at the site of primordium formation, i.e. the direction of bulging of the SAM surface accompanying leaf primordium formation is nearly parallel to the shoot axis (upward bulging).

Later on, during the separation stage (Fig. 4A, the second and the third reconstruction), growth at the SAM, between the meristem centre and the future primordium boundary, is still virtually nil but, unlike in the preceding stage, there is no change in meristem shape between these two points, meaning there is also virtually no growth in the anticlinal direction. Local growth in the meridional direction between the future boundary and primordium tip is also rather small; however, there are some important changes in the geometry of this region, which is displaced upward with respect to the meristem flanks. Since there is no displacement at the meristem centre and the primordium boundary, this presumably is a manifestation of growth in the anticlinal direction, in this case leading to upward bulging at the SAM periphery. Consequently, the shape of the apex profile in the region around the boundary between the SAM and primordium changes from nearly straight to concave. The concave shape of this part of the profile is also visualized in curvature plots where the curvature of the saddle-shaped adaxial primordium boundary is negative in the meridional direction.

Once the separation stage is completed (Fig. 4B), the cell on the primordium boundary is displaced further and further away from the SAM centre. This is a manifestation of the strong local growth in the meridional direction accompanying rebuilding of the peripheral zone of the SAM. The outline of this portion of the SAM becomes

more curved than in the preceding stages. Simultaneously the cell located on adaxial primordium flanks (labelled with 'p') is also displaced, both away from the SAM axis and parallel to the axis (upward). When interpreting such a displacement one should keep in mind that the two profiles are overlaid with the SAM centre as a reference point, while the cell at the primordium boundary is strongly displaced. The observed displacement of a cell located at adaxial primordium flanks (cell 'p') is presumably due to expansion of the adaxial primordium surface and a change of primordium inclination to nearly parallel to the SAM axis. During the next stage, i.e. the primordium curving stage (Fig. 4C), the adaxial primordium boundary is displaced still further from the meristem centre, and the outline of the meristem periphery changes to still more curved, which probably is the early manifestation of initiation of a new primordium in the adjacent portion of the periphery (the last reconstruction in Fig. 4C). The earlier formed primordium slowly curves over the SAM (the first two reconstructions in Fig. 4C).

In the reproductive apex (Fig. 5), early stages of bract primordium formation, i.e. from the initial bulging to the end of the separation stage, closely resemble those of vegetative leaf primordium (compare Fig. 5A and Fig. 4A, B). At the onset of flower primordium formation, i.e. at the beginning of lateral bulging, a strong displacement of cells located at the SAM periphery (dots 'bf' and 'f' in Fig. 5B, the first two reconstructions) and at the boundary between

the meristem and the bract primordium (dot 'bp') takes place. The direction of this displacement is nearly tangential to the SAM outline. The general shape of the profile of this SAM portion does not change much, but growth of the peripheral zone in the meridional direction is apparent at this stage, especially in a region closer to the SAM centre (note that the lengths of all the displacement segments is similar, meaning that the dots located further from the SAM centre were displaced mainly due to the growth between the centre and the closest dot). Later on during the lateral bulging and early separation of the flower primordium (Fig. 5B, the second and third reconstructions), the intensive growth in the meridional direction of the peripheral zone is maintained, but simultaneously the shape of the SAM periphery changes from nearly flat to slightly concave, as the saddle-like adaxial flower primordium boundary (dot 'bf') appears. The displacement of all the labelled cells is in a direction nearly perpendicular to the shoot axis. Judging from the increasing lengths of displacement segments, growth in the meridional direction takes place along the whole SAM periphery. Since at this stage the base of the bract subtending the flower primordium (asterisk) is displaced relatively little from the SAM centre, the flower primordium seems to grow quickly on the slowly growing bract base.

During the late separation stage (Fig. 5B, the third and fourth reconstruction), the position of cells remains nearly fixed. Only the cell located at the adaxial flower primordium
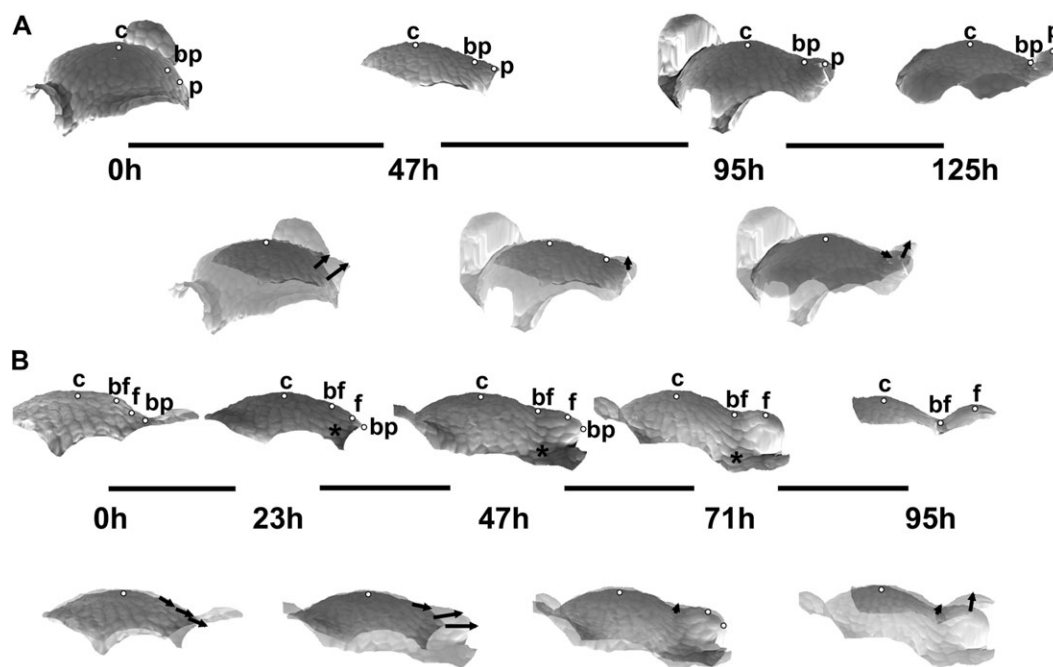

Fig. 5. Sequences of 3D reconstructions of replicas taken from two individual shoot apices of *Anagallis arvensis* in the reproductive developmental phase, representing consecutive stages of bract and flower primordium development: initial bulging, lateral expansion, and separation stages of bract primordium development (A); lateral bulging, separation, and axil deepening stages of flower primordium development (B). White dots on the profiles point to: c, the cell on the top of the SAM; bp, the cell at the boundary between the meristem and bract primordium; p, the cell on the bract primordium tip; bf, the cell at the boundary between the flower primordium and the SAM; and f, the cell at the tip of the flower primordium. Asterisks point to the cell at the base of the bract subtending the flower primordium. Other labelling is as in Fig. 4.

boundary (dot 'bf') is slightly displaced downward, while a local change in curvature takes place and a distinct crease is formed on a previously nearly flat region. At the same time, the growth of flower primordium is slowed down. Eventually, the adaxial flower primordium boundary remains nearly fixed, while flower primordium grows upwards rather than laterally (Fig. 5B, the last two reconstructions), presumably because of the presence of the bract that limits lateral growth (not shown in this profile).

Discussion

Changes of growth and geometry accompanying formation of different primordium types at the SAM of Anagallis arvensis

In *Anagallis* during the vegetative phase only leaf primordia are formed at the SAM periphery, in contrast to the SAM in the reproductive phase where flower primordia are also formed at the SAM periphery, in the future axil of the subtending primordium of the leaf-like bract. Both the SAM and the future axil of the bract subtending the flower contribute to flower primordium formation. As a consequence, at the *Anagallis* SAM in the reproductive phase, two primordia are formed one after and above the other, along the meristem meridian. The first one is bract and the second is the flower primordium (Green *et al.*, 1991).

Based on computation of growth (strain) rate and the curvature of the *Anagallis* shoot apex surface in the vegetative phase, four stages in early leaf primordium development can be distinguished (Kwiatkowska and Dumais, 2003): the initial bulging of SAM periphery; lateral expansion of the primordium; separation of the primordium from the SAM; and primordium curving (bending) over the SAM. Formation of the bract at the SAM periphery in the reproductive phase is generally similar to leaf primordium formation in both geometry and growth characteristic over consecutive developmental stages. The difference is that the lateral expansion stage is less distinct in the case of the bract primordium. Moreover, the bract primordium starts to grow over the SAM much later than the vegetative leaf primordium. This is because the bract primordium is apparently displaced by the emerging flower primordium.

The bract primordium and the flower primordium, both formed at the SAM periphery during the reproductive phase, exhibit a striking and sometimes confusing similarity in shapes during the early stages of their development. There are, however, major differences in their formation. Firstly, areal growth rates at the earliest stage of flower primordium formation are higher than at the site of bract formation. Secondly, growth at the flower formation site is strongly anisotropic, unlike in the bract primordium. Also no lateral expansion takes place in the course of flower primordium formation, but, on the contrary, the direction of maximal growth rate remains meridional for a relatively long time, until growth becomes less anisotropic. Since up to this stage the flower primordium still rather closely resembles the bract primordium, the development of the two primordium types in *Anagallis* provides a good example of how very different growth can accompany formation of structures that are very similar in shape. This is an important argument in support of the need to quantify local geometry and growth (Silk, 1984). It is known that a given shape can be maintained by various growth patterns (Green *et al.*, 1970). The present case is an example on two different modes of *de novo* formation of a given shape. The reported differences, however, are in the growth pattern on the surface and growth in the anticlinal direction, i.e. the most important direction for surface bulging, is not accounted for.

Two ways to form an adaxial primordium boundary

The way in which two types of boundaries (future axils) between a primordium and the SAM are formed can also be studied at the SAM of *Anagallis*. These are the boundary between the SAM and the leaf or bract primordium, and that between the SAM and the flower primordium. The growth accompanying formation of the two types of boundaries is strikingly different. In the case of the bract boundary, similar to the earlier described leaf boundary (Kwiatkowska and Dumais, 2003), growth accompanying its formation is very slow (low areal growth rate) and strongly anisotropic. Maximal growth rates are in the latitudinal direction, while they are minimal in the meridional direction, where no growth or even contraction has been noted (Kwiatkowska and Dumais, 2003). The adaxial flower primordium boundary is characterized by entirely different growth at the onset of the separation stage. Together with the adjacent portion of the SAM periphery and the emerging flower primordium, the site of boundary formation comprises the fastest growing region of the apex. Growth in this region is strongly anisotropic, but with the maximal growth rate direction being meridional. Examination of the geometry reveals that the boundary first appears as a narrow ridge and only later is the narrow deep crease formed. Only then does growth at the adaxial flower primordium boundary become similar to that at the bract primordium boundary (the future axil).

Two methods of boundary formation have been described previously for the *Arabidopsis* inflorescence SAM (Kwiatkowska, 2006). In this species, however, slow growth at the future boundary, which is typical for *Anagallis* leaf or bract, accompanies the formation of flower primordium proper, while fast growth is typical for rudimentary bract. It is known that at the adaxial primordium boundary cell divisions are suppressed. In *Arabidopsis* SAM these regions are distinguished by the expression of *CUP-SHAPED COTYLEDONS* (*CUC*) genes (Breuil-Broyer *et al.*, 2004; Aida and Tasaka, 2006). It may therefore be critical to follow simultaneously the expression patterns of *CUC* genes, growth, and geometry changes in *Arabidopsis* in order to verify the role of *CUC* genes in division suppression at boundaries of various organ types.

Self-perpetuation at the inflorescence SAM in comparison with the vegetative SAM

According to Vaughan (1955) and Brulfert (1962) the cytohistological zonation of the vegetative SAM of *Anagallis* is distinct. Thus the central region of slower growth observed on the vegetative SAM surface possibly represents the surface of the central zone. Vaughan (1955) reported that similar cytohistological zonation is also characteristic for the inflorescence SAM of *Anagallis*, but that it is less distinct. Also the growth rate distribution on the inflorescence SAM surface does not imply the existence of distinct central and peripheral zones. The present study shows the presence of a slowly growing region in the central part of the SAM surface, but the position of this region is not stable with respect to cells. Also the growth pattern of the SAM periphery is not uniform. In particular, in some regions of the SAM periphery at certain time intervals, growth is as slow as in the central part of the SAM. It could be expected that averaging of such a growth pattern at longer time intervals would give zones of slower and faster growth that are not strongly pronounced.

The changes in location of the slowly growing region on the examined inflorescence SAMs may be related to spiral phyllotaxis. One may expect that the growth pattern is more complex and asymmetric in the case of spiral than in decussate phyllotaxis, especially if a flower primordium is formed when the subtending bract primordium is still contacting the SAM flanks. The inflorescence SAM zonation observed by Vaughan (1955) may thus also be due to the fact that he examined SAMs exhibiting decussate phyllotaxis.

The inflorescence *Anagallis* SAM (present investigation) resembles that of *Arabidopsis* (Kwiatkowska, 2004*a*) in that the location of the slowly growing region is not exactly symmetric around the SAM centre and in that this location changes with respect to cells. In the *Arabidopsis* inflorescence SAM the differentiation of the surface into slow and fast growing zones is still less apparent than in *Anagallis*. A reason for this may, among others, be the small number of cells comprising the SAM and the variation of cell cycle parameters among individual meristems (Grandjean *et al.*, 2004; Kwiatkowska, 2008). Moreover, the growth of the inflorescence SAM in *Arabidopsis* is more determinate than in *Anagallis*. Thus the stronger activation of the central zone and, accordingly, the disappearance of differences between the central and peripheral zones may be expected in *Arabidopsis* rather than in *Anagallis*.

Sequential 3D reconstructions of an individual apex surface

The method of sequential replicas employed here is sufficient for computation of growth rates at the shoot apex surface, but does not provide empirical data for direct computation of growth of the apex interior (Dumais and Kwiatkowska, 2002). The 3D reconstruction of the apex surface, however, allows one to draw some indirect conclusions on growth within the apex. In particular, the directions of bulging of the apex surface accompanying formation of primordia exhibiting different identities can be judged.

In *Anagallis* shoot apices, both leaf and bract primordia are formed due to bulging in the direction nearly parallel to the shoot axis, while the flower primordium bulges initially in a direction perpendicular to the axis. Interestingly, this is opposite to what has been observed in *Arabidopsis* (Kwiatkowska, 2006) where bulging during rudimentary bract formation is similar to that of flower primordium formation in *Anagallis*. Bulging during flower primordium formation in *Arabidopsis* is in a direction similar to that during bract formation in *Anagallis*. However, Vaughan (1955) has shown that the first periclinal divisions accompanying leaf primordium formation are the same in *Arabidopsis* and *Anagallis*. The same is also true for flower primordia. This may be yet another argument against the significance of the periclinal divisions in primordium formation (Lyndon, 1998).

The method of dense 3D reconstruction employed in the present investigation could be used further to assess and quantitatively analyse the displacement velocity fields of marker points on the apex surface, though such an analysis would need to combine the Lagrangian and Eulerian approaches (Silk, 1984). Until now the available data on apex growth are either exclusively on the apex surface (Green *et al.*, 1991; Dumais and Kwiatkowska, 2002; Grandjean *et al.*, 2004; Reddy *et al.*, 2004) or are based only on longitudinal meristem sections (Lyndon, 1998; reviewed in Kwiatkowska, 2004*b*). As a result, our knowledge on the growth pattern at the shoot apex is incomplete. Combining the surface growth computation with the assessment of displacement velocity fields may to certain extent fill this gap.

References

Aida M, Tasaka M. 2006. Morphogenesis and patterning at the organ boundaries in the higher plant shoot apex. *Plant Molecular Biology* **60,** 915–928.

Arun KS, Huang TS, Blostein SD. 1987. Least-squares fitting of two 3-D point sets. *IEEE Transactions on Pattern Analysis and Machine Intelligence* **9,** 698–700.

Ballard LAT. 1969. *Anagallis arvensis* L. In: Evans LT, ed. *The induction of flowering*. Australia: Macmillan, 376–392.

Battey NH, Lyndon RF. 1990. Reversion of flowering. *Botanical Review* **56,** 162–189.

Bernier G. 1988. The control of floral evocation and morphogenesis. *Annual Review of Plant Physiology and Plant Molecular Biology* **39,** 175–219.

Breuil-Broyer S, Morel P, de Almeida-Engler J, Coustham V, Negrutiu I, Trehin C. 2004. High-resolution boundary analysis during *Arabidopsis thaliana* flower development. *The Plant Journal* **38,** 182–192.

Brulfert J, Fontaine D, Imhoff C. 1985. *Anagallis arvensis*. In: Halevy AH, ed. *CRC handbook of flowering*. Boca Raton, FL: CRC Press, 334–349.

Brulfert J. 1962. Structure et fonctionnement du point végétatif d'*Anagallis arvensis* L. ssp *phoenicea* Scop. en jours courts. *Comptes Rendus de l'Académie des Sciences* **254,** 1475–1477.

Corson GE. 1969. Cell division studies of the shoot apex of *Datura stramonium* during transition to flowering. *American Journal of Botany* **56,** 1127–1134.

Cutter EG. 1971. *Plant anatomy: experiment and interpretation. Part 2. Organs*. London: Edward Arnold (Publishers) Ltd.

Dumais J, Kwiatkowska D. 2002. Analysis of surface growth in shoot apices. *The Plant Journal* **31,** 229–241.

Grandjean O, Vernoux T, Laufs P, Belcram K, Mizukami Y, Traas J. 2004. *In vivo* analysis of cell division, cell growth, and differentiation at the shoot apical meristem in *Arabidopsis*. *The Plant Cell* **16,** 74–87.

Green PB, Havelange A, Bernier G. 1991. Floral morphogenesis in *Anagallis*: scanning-electron-micrograph sequences from individual growing meristems before, during, and after the transition to flowering. *Planta* **185,** 502–512.

Green PB, Erickson RO, Richmond PA. 1970. On the physical basis of cell morphogenesis. *Annals of the New York Academy of Sciences* **175,** 712–731.

Hepworth SR, Klenz JE, Haughn GW. 2006. UFO in the *Arabidopsis* inflorescence apex is required for floral-meristem identity and bract suppression. *Planta* **223,** 769–778.

Kwiatkowska D. 1995. Ontogenetic changes of phyllotaxis in *Anagallis arvensis* L. *Acta Societatis Botanicorum Poloniae* **64,** 319–325.

Kwiatkowska D. 1997. Intraspecific variation of phyllotactic stability in *Anagallis arvensis*. *Acta Societatis Botanicorum Poloniae* **66,** 259–271.

Kwiatkowska D. 2004*a*. Surface growth at the reproductive shoot apex of *Arabidopsis thaliana*: *pin-formed 1* and wild type. *Journal of Experimental Botany* **55,** 1021–1032.

Kwiatkowska D. 2004*b*. Structural integration at the shoot apical meristem: models, measurements and experiments. *American Journal of Botany* **91,** 1277–1293.

Kwiatkowska D. 2006. Flower primordium formation at the *Arabidopsis* shoot apex: quantitative analysis of surface geometry and growth. *Journal of Experimental Botany* **57,** 571–580.

Kwiatkowska D. 2008. Flowering and apical meristem growth dynamics. *Journal of Experimental Boany* **59,** 187–201.

Kwiatkowska D, Dumais J. 2003. Growth and morphogenesis at the vegetative shoot apex of *Anagallis arvensis* L. *Journal of Experimental Botany* **54,** 1585–1595.

Laufs P, Grandjean O, Jonak C, Kiêu K, Traas J. 1998. Cellular parameters of the shoot apical meristem in *Arabidopsis*. *The Plant Cell* **10,** 1375–1389.

Long J, Barton MK. 2000. Initiation of axillary and floral meristems in *Arabidopsis*. *Developmental Biology* **218,** 341–353.

Lyndon RF. 1998. *The shoot apical meristem*. Cambridge: Cambridge University Press.

Lyndon RF, Battey NH. 1985. The growth of the shoot apical meristem during flower initiation. *Biologia Plantarum* **27,** 339–349.

Marc J, Palmer JH. 1984. Variation in cell cycle time and nuclear DNA content in the apical meristem of *Helianthus annuus* L. during the transition to flowering. *American Journal of Botany* **71,** 588–595.

Reddy GV, Heisler MG, Ehrhardt DW, Meyerowitz EM. 2004. Real-time lineage analysis reveals oriented cell divisions associated with morphogenesis at the shoot apex of *Arabidopsis thaliana*. *Development* **131,** 4225–4237.

Romberger JA, Hejnowicz Z, Hill JF. 1993. *Plant structure: function and development*. Berlin: Springer Verlag.

Routier-Kierzkowska A-L, Kwiatkowska D. 2008. New stereo-scopic reconstruction protocol for scanning electron microscope images and its application to *in vivo* replicas of the shoot apical meristem. *Functional Plant Biology* **35,** 1034–1046.

Silk WK. 1984. Quantitative descriptions of development. *Annual Review of Plant Physiology* **35,** 479–518.

Tooke F, Ordidge M, Chiurugwi T, Battey N. 2005. Mechanisms and function of flower and inflorescence reversion. *Journal of Experimental Botany* **56,** 2587–2599.

Vaughan JG. 1955. The morphology and growth of the vegetative and reproductive apices of *Arabidopsis thaliana* (L.) Heynh., *Capsella bursa-pastoris* (L.) Medic. and *Anagallis arvensis* L. *Journal of the Linnean Society, London (Botany)* **55,** 279–301.

Weberling F. 1989. *Morphology of flowers and inflorescences*. Cambridge: Cambridge University Press.

Williams MH, Green PB. 1988. Sequential scanning electron microscopy of a growing plant meristem. *Protoplasma* **147,** 77–79.

Williams MH. 1991. A sequential study of cell divisions and expansion patterns on a single developing shoot apex of *Vinca major*. *Annals of Botany* **68,** 541–546.